

PERFORMANCE AND PARAMETERS OF A NOVEL TALBOT EFFECT CONFOCAL RESONATOR FOR MM-WAVE FEL

H. S. Marks*, J. Dadoun, O. Faingersh, K. Garb, A. Gover, Tel-Aviv University
B. Kapilevich, B. Litvak, Ariel University Centre of Samaria, Ariel

Abstract

The design, operating principles, and results of characterization for a novel resonator are outlined. Measurements were conducted prior to insertion into the Wiggler cavity for future testing under lasing. The W-band (75-110 GHz) resonator consists of two Talbot splitters and two confocal parabolic mirrors for decoupling the electron beam from the RF radiation, a corrugated waveguide, and an adjustable three grid reflector system. Two degrees of freedom have been built into the grid system, firstly, the central grid can be rotated via remote control to alter the out-coupling coefficient, and secondly, also using a motor it is possible to remotely move the grid system back and forth altering the length of the resonator allowing continuous tuning of the longitudinal mode resonant frequencies (spaced about 100MHz apart). The radiation pattern of the resonator mode is nearly a Gaussian. The input reflectance and Q factors were measured by matching the S parameters of the device (measured with a Scalar Network Analyser) to the theoretical Fabry-Perot resonator reflection and transmission curves. Based on this estimate the roundtrip losses of the tunable resonator are 37%.

OVERVIEW OF NEW SYSTEM

The completion of all the parts of the new resonator designed for the Israeli EA FEL has allowed for testing the complete system before insertion into the Wiggler and wider system. The curved parallel plate (CPP) waveguide that was previously used has been replaced with a corrugated waveguide of height 10.7 mm and width 15 mm. It has been calculated that this should reduce losses in the system. Both the CPP and Corrugated waveguide were designed according to the dispersion relation such that the fundamental mode TE_{01} would interact with the beam energy of the system (1.4 MeV). The roundtrip losses in the 890 mm long over-moded corrugated waveguide were measured to be 4.5%.

Connected to the entrance of the waveguide is a Talbot splitter [1] (see figure 1). The Talbot splitter consists of a rectangular waveguide section with a width of $a = 25$ mm, and a height of 10.7 mm. The electron beam which passes through the resonator, travelling along the z-axis enters via a window which is bolted on to the front face of the rectangular Talbot section (left most side of figure 1). The window is large enough to allow the electron beam to enter (10.7 mm height, 10 mm width), but reflects the radiation built up in the resonator. The reflection occurs due to the Talbot imaging effect which arises due to the interference of the different modes in the rectangular

Talbot waveguide, which are excited from the right by the single (fundamental) mode of the corrugated waveguide (see Fig. 1). In a rectangular waveguide at a distance of $L = 8a^2/\lambda$ any initial image is re-formed (where a is the width of the waveguide and λ is the radiation wavelength). For a symmetric image this occurs at $L = 2a^2/\lambda$. The image is symmetrically split about the vertical (y) axis for $L = a^2/\lambda$. The Talbot splitter is made of a rectangular waveguide of this length. This allows the beam and wave to be effectively de-coupled. The combined losses of the Talbot splitter and corrugated waveguide were measured to be 5.91%.

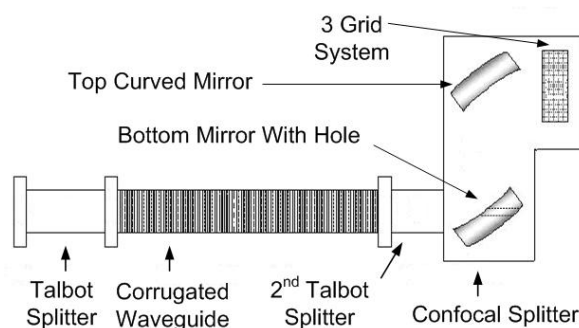


Figure 1: A schematic overview of the main components of the resonator. The electrons travel from $-z$ (left) to $+z$ (right) through the resonator.

On the other end of the resonator the confocal splitter also serves to de-couple the radiation from the electron beam. An opening in the bottom curved mirror [2] (see figure 1) allows the electron beam to pass through, whilst the radiation pattern is again split to either side of the opening. The image is re-formed at the middle grid of the 3 grid system after reflecting off the top mirror. The two parabolic mirrors were designed to minimise dispersion. An external view of the confocal splitter is shown in figure 2. A small motor controls the position of a shield which can be lowered to protect the bottom mirror during initial operation of the laser when the beam trajectories are verified. Once transport is satisfactory the shield can be raised.

A second motor is attached to the carriage of the 3-grid system and can move up to 3 mm, lengthening or shortening the resonator. This should allow high resolution sub-MHz continuous tuning.

Finally, the 3-grid system which replaced a single fixed grid consists of two fixed grids aligned to allow maximum transmission of the TE_{01} mode, and one motor-controlled central grid capable of rotating through 90° and thus varying the transmission coefficient from 0 to 1.

* Corresponding author. Email: harry@eng.tau.ac.il

Each grid is formed by tungsten wires supported within a copper frame. The grids are separated by $\lambda/8$ mm where $\lambda = 3$ mm [3]. The principal advantage conferred by this upgrade is the ability to vary the power coupled out of the resonator.

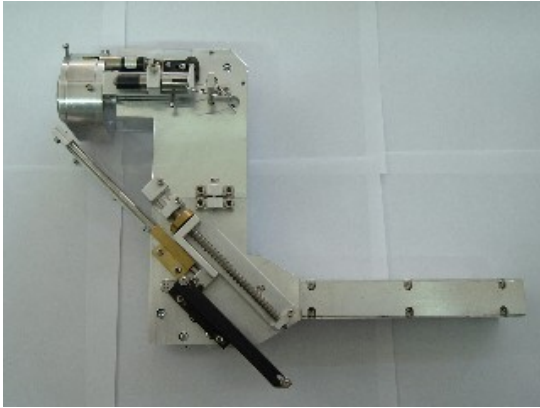


Figure 2: External view of the confocal splitter system.

The theoretical losses for the confocal splitter part of the resonator system were estimated to be 12%. In practice losses were as high as 29.6%. One third of this loss can be attributed to the 3 grid system.

DETERMINATION OF LOSSES

A Fabri-Perot resonator was formed from the different components of the resonator by attaching a mode exciter and grid to the different parts (the grid had a power reflectivity of 92%). A Scalar Network Analyser was used to measure the power reflectivity from 99.8-100.2 GHz with the mode exciter connected. In each case the reference for determining the absolute value of S_{11} was a short positioned in place of the grid. The experimental curves were matched to theoretical curves of a Fabri-Perot resonator [4]:

$$\Gamma = |S_{11}| = \frac{(r_1 - \tau r_2)^2 + 4\tau r_1 r_2 \sin^2(\delta/2)}{(1 - \tau r_1 r_2)^2 + 4\tau r_1 r_2 \sin^2(\delta/2)} \quad (1)$$

Where the power reflectivity Γ is a function of r_1 and r_2 , the reflected amplitudes from the grid at the end of the mode exciter and the end-point of the particular part being measured. The round trip amplitude transmission coefficient through the system (excluding the end mirrors) is given by τ and δ denotes the phase shift of the wave.

The round trip losses of the element are determined once the parameter τr_2 is evaluated from the matching of the theoretical and experimental curves:

$$L = 1 - R_{RT} = 1 - (\tau r_2)^2 \quad (2)$$

An example of such matching is shown in figure 3. The particular measurement shown was of the waveguide and confocal system with a short positioned in place of the 3-grid system. Losses were calculated to be ~27%.

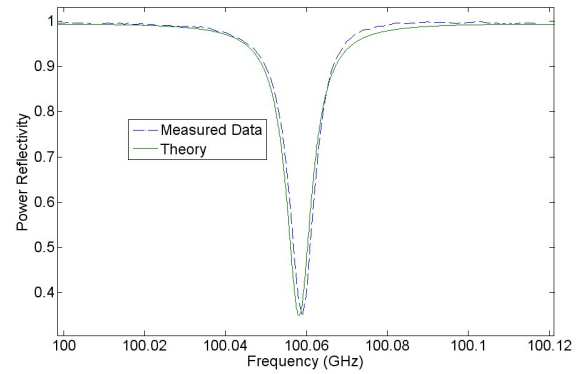


Figure 3: Power reflectivity as a function of frequency without the straight Talbot section and rotating grids.

CONCLUSION

Total measured losses are higher than expected at 37% as a result of the rotating grid system. However, the system is functional and is expected to provide new lasing capabilities based on the new degrees of freedom built in.

REFERENCES

- [1] G. G. Denisov, D. A. Lukovikov, and M. Yu. Shmelyov, "Microwave Systems Based on the Effect of Image Multiplication in Oversized Waveguides", *Proceedings of SPIE - The International Society for Optical Engineering*, v 2104, p 485-486, 1993
- [2] M. Kesselbrener, S. Ruschin, B. Lissach, A. Gover, "Numerical studies of resonators with on-axis holes in mirrors for FEL applications", *Nuclear Instruments and Methods in Physics Research, A* 304, 1991, 782-785
- [3] B. Kapilevich, O. Faingersh, and A. Gover, "Accurate determination of Q-factor of a quasi-optical resonator", *Microwave and Optical Tech Letters*, Vol. 36, No. 4, 2003.
- [4] Haus, H. "Waves and Fields in Optoelectronics". Prentice-Hall, 1984.